Quantifying CanESM5 and EAMv1 sensitivities to volcanic forcing for the CMIP6 historical experiment

Landon A Rieger[1], Jason NS Cole[2], John C Fyfe[2], Stephen Po-Chedley[3], Philip J Cameron-Smith[3], Paul J Durack[3], Nathan P Gillett[2], and Qi Tang[3]

[1]Institute of Space and Atmospheric Studies, University of Saskatchewan, Saskatoon, SK
[2]Canadian Centre for Climate Modelling and Analysis, Environment Canada, Victoria, BC
[3]Lawrence Livermore National Laboratory, Livermore, California

Correspondence: Landon Rieger (landon.rieger@usask.ca)

Abstract. Large volcanic eruptions reaching the stratosphere have caused marked perturbations to the global climate including cooling at the Earth's surface, changes in large-scale circulation and precipitation patterns and marked temporary reductions in global ocean heat content. Many studies have investigated these effects using climate models, however uncertainties remain in the modelled response to these eruptions. This is due in part to the diversity of forcing datasets that are used to prescribe the

5   distribution of stratospheric aerosols resulting from these volcanic eruptions, as well as uncertainties in optical property derivations from these datasets. To reduce these uncertainties in the Coupled Model Intercomparison Project 6 (CMIP6) a combined stratospheric aerosol dataset, the Global Space-based Stratospheric Aerosol Climatology, GloSSAC, was constructed. Along with information from ice-cores and sun photometers, GloSSAC was used to generate aerosol distributions, characteristics and optical properties and construct a consistent stratospheric aerosol forcing dataset for models participating in CMIP6. This "ver-

10   sion 3" of the stratospheric aerosol forcing has been endorsed for use in all contributing CMIP6 simulations. Recent updates to the underlying GloSSAC from version 1 to version 1.1 affected the 1991 to 1994 period and necessitated an update to the stratospheric aerosol forcing from version 3 to version 4. As version 3 remains the official CMIP6 input, quantification of the impact on radiative forcing and climate is both relevant and timely for interpreting results from experiments such as the CMIP6 historical simulations. This study uses the Canadian Earth System Model version 5 (CanESM5) to estimate the difference in

15   instantaneous radiative forcing in simulated post-Pinatubo climate response when using version 4 instead of version 3. Differences in temperature, precipitation, and radiative forcings are generally found to be small compared to internal variability. To further elucidate sensitivities that are representative of the CMIP6 model suite, additional simulations are performed using the Energy Exascale Earth System Model (E3SM) Atmosphere Model version 1 (EAMv1), which also indicates that the impact of the update to GloSSAC version 4 on climate are relatively minor. An exception to this is differences in temperature anomalies

20   in the stratosphere, which can be as large as 3°C following the eruption of Mt. Pinatubo.

1 Introduction

The stratosphere holds a layer of aerosols consisting primarily of sulfuric acid and water that impact climate in a variety of ways (Kremser et al., 2016). Most importantly, this stratospheric aerosol layer scatters incoming light leading to a cooling effect.

Scattering in the atmosphere can be greatly enhanced by volcanic eruptions, multiplying the impact on climate. For example, the 1991 eruption of Mt. Pinatubo injected an estimated $10\,\text{Tg}$ of sulfur into the stratosphere (Guo et al., 2004), resulting in a peak top-of-atmosphere radiative forcing of roughly 3-4 Wm^{-2} (Ramachandran et al., 2000; Hansen et al., 1992), and cooled global temperatures by a few tenths of a degree Celsius (Robock and Mao, 1995; Thompson and Solomon, 2009). The impact

5 on oceans was equally impressive, with global ocean heat content decreasing by $3 \times 10^{22}\,\text{J}$, and sea level decreasing by $5\,\text{mm}$ (Church et al., 2005). Over the last two decades a number of smaller volcanic eruptions have also injected sulfur dioxide into the stratosphere (Vernier et al., 2011). These eruptions have had a small but discernible effect on global temperature (Solomon et al., 2011; Fyfe et al., 2013; Haywood et al., 2014; Santer et al., 2014).

Issues remain in characterizing the radiative forcing caused by changes in stratospheric aerosols and the climate responses

10 that result. General circulation models, for example, often overestimate the stratospheric warming response following the eruption of Mount Pinatubo (Lanzante and Free, 2008; Gettelman et al., 2010). The impact of smaller, post-Pinatubo volcanic eruptions on surface cooling needs better quantification (Santer et al., 2014), and large uncertainties remain in characterizing the response of the upper troposphere and lower stratosphere to volcanic eruptions (Ridley et al., 2014; Andersson et al., 2015). Such uncertainties in the climate response to volcanic eruptions result in part from differences in the stratospheric

15 aerosol datasets that are prescribed in general circulation models (GCMs). GCMs participating in the Fifth Coupled Model Intercomparison Project (CMIP5) (Taylor et al., 2012; Driscoll et al., 2012) used stratospheric aerosol datasets from Ammann et al. (2003) and Sato et al. (1993), while post-CMIP5 simulations (Solomon et al., 2011; Fyfe et al., 2013) have used datasets that include recent eruptions (Vernier et al., 2011). To avoid a diversity of stratospheric aerosol datasets, and their associated forcings, a homogenized stratospheric aerosol time series was developed for use with CMIP6 (Durack et al., 2018).

20 This stratospheric aerosol dataset will help reduce uncertainties that have resulted from differing stratospheric aerosol assumptions (e.g., in CMIP5). While modelling centres were performing simulations for CMIP6 an update was made to this dataset that affected the stratospheric aerosol loading of the Pinatubo eruption. Although the updates are not CMIP6 endorsed, and forcing should remain consistent across models, the changes to aerosol loading can be substantial. To estimate the potential effect of these changes on CMIP6 results we characterize the impact of this dataset update on the global climate using two

25 general circulation models.

2 The Stratospheric Aerosol Dataset

For CMIP6 experiments the stratospheric aerosol forcing dataset post-1980 was constructed in a two step process. First, data from multiple satellite instruments was compiled into a continuous extinction record at $525\,\text{nm}$ that spans the entire period. Extinction measurements at other visible and near-infrared wavelengths are available for portions of the record, but do not

30 span its entirety. This composes the Global Satellite-based Stratospheric Aerosol Climatology, or GloSSAC (Thomason et al., 2018). The second step is deriving the asymmetry factor, single scattering albedo and extinction at the wavelengths required for radiative transfer calculations in climate models (Luo, 2018a). This was done by deriving a particle size distribution from the measurement periods where multiple wavelengths are available (1985-2005) and extrapolating to periods where they are not

(pre-1985 and post-2005). This composes the IACETH-SAGE3lambda-3-0-0 dataset available from input4MIPs. Luo (2018a) then used the particle size distributions to compute the optical parameters at the wavelength bands of participating models. In this way, the optical properties required for each participating model's radiative transfer scheme are consistent with the underlying extinction and particle size climatology. As of May 31, 2016 these were available from `ftp://iacftp.ethz.`
5 `ch/pub_read/luo/CMIP6` and represented version 3 stratospheric aerosol datasets used for CMIP6, herein referred to as version 3, or 'v3' for brevity.

After publication of these datasets an error was found in the GloSSAC processing necessitating an update to version 4 (Luo, 2018b). The update was published August 27, 2018 and is available from `ftp://iacftp.ethz.ch/pub_read/`
`luo/CMIP6_SAD_radForcing_v4.0.0`. As it is not yet officially CMIP endorsed it is not currently available from
10 input4MIPs. Changes to the data processing primarily affected only a subset of the satellite measurements which contributed to the January 1991 to December 1994 period, so data outside of this range remains the same between version 3 and version 4.

Of most direct consequence to GCM experiments is the stratospheric aerosol optical depth (SAOD), calculated as the vertical integral of aerosol extinction from the tropopause to the top of the atmosphere, or in this case to the top of the dataset at 40 km. The top panel in Figure 1 shows the monthly SAOD at 550 nm from the version 3 dataset. The impact of the Mount Pinatubo
15 eruption on SAOD is largest in the tropics, but a substantial amount of aerosol is transported to the extra-tropics in both hemispheres in ensuing months, and global SAOD values remain elevated over background for several years. The bottom panel shows the SAOD differences between version 3 and version 4. The peak Pinatubo-induced SAOD values are smaller in version 4, but v4 exhibits modest increases at other locations, reducing globally averaged differences and potentially offsetting climate differences between versions. Fractional differences show a very similar pattern with differences in the thickest part of
20 the plume reaching 20%, and differences nearer the poles reaching 50% for short periods of time.
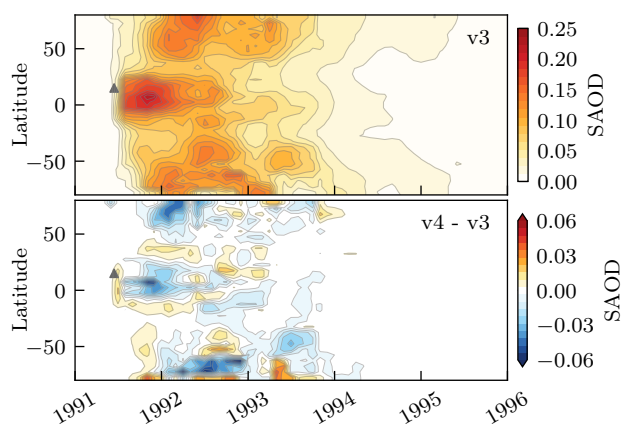
Figure 1. The top panel shows aerosol optical depth in the stratosphere (SAOD) at 550 nm from the v3 dataset. The bottom panel shows the absolute difference between the versions, computed as v4 − v3, during this same time period. The triangle marks the Pinatubo eruption at 14°N on June 15, 1991.

However, when looking at SAOD alone, decreases in extinction at higher altitudes can be offset by increases nearer the tropopause, reducing the apparent differences. This can be seen in Figure 2, which shows the difference in extinction at 550 nm as a function of altitude and time for the global average and three latitude bands that showed large changes in SAOD. The most prominent differences between v3 and v4 are evident in the tropics where the main aerosol plume has been reduced in thickness

5 by up to 50%. Conversely, altitudes below the main plume have increased extinction. While the increase extends to the ground, most of these altitudes are below the tropopause, and so are not considered in climate simulations (CMIP6 simulations are recommended to use stratospheric aerosols only above the tropopause (Thomason et al., 2018)). The solid gray lines in Figure 2 indicate the monthly averaged thermal tropopause from NCEP1 reanalysis data (Kalnay et al., 1996).
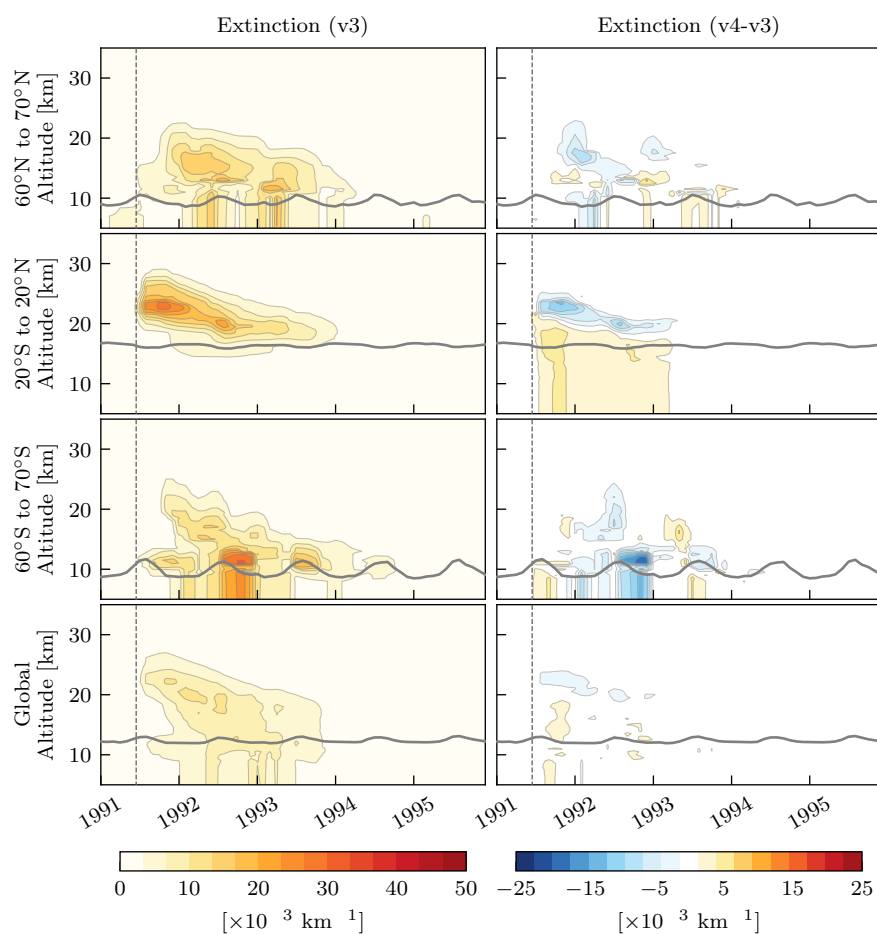
Figure 2. The left column shows the version 3 extinction at 550 nm in four latitude bands. The right column shows the change in extinction when the newer version 4 data product is used (v4-v3). The solid gray lines show the monthly NCEP1 thermal tropopause and the dashed line indicates the date of the Pinatubo eruption.

3 Models

3.1 CanESM5

The Canadian Earth System Model version 5 (CanESM5) was used to evaluate the effect of the change from version 3 to version 4 of the aerosol dataset on the post-Pinatubo instantaneous radiative forcing and climate simulated by this model. We provide here a brief description of CanESM5 but a more through overview of the components and properties of CanESM5 is given in Swart et al. (2019). The atmospheric component of CanESM5, the Canadian Atmospheric Model version 5 (CanAM5) is a spectral model employing T63 triangular truncation with physical tendencies calculated on a 128×64 (∼2.81°) horizontal linear grid. CanAM5 has 49 unevenly spaced vertical levels up to ∼0.1 hPa. The physical ocean component of CanESM5 is based on NEMO version 3.4.1 (Madec and Imbard, 2012) and has 45 levels with approximately 6 m resolution in the upper ocean increasing to ∼250 m in the lower ocean, and a horizontal resolution of approximately 1°.

3.2 EAMv1

In addition to CanESM5, we also consider simulations from version 1.0 of the Energy Exascale Earth System Model (E3SM) (Golaz et al., 2019). In particular, we employ the E3SM Atmosphere Model version 1 (EAMv1) (Rasch et al., 2019) using prescribed sea surface temperature (SST) and sea ice concentrations as boundary conditions. SST and sea ice fields are from HadISST version 1.1.3 (Durack and Taylor, 2017) as described in Hurrell et al. (2008). The model solves the atmospheric primitive equations using a continuous Galerkin spectral finite element method and has a horizontal resolution of approximately 100 km at the equator. EAMv1 has 72 unevenly spaced vertical levels with a model top at ∼0.1 hPa, and employs a linearized ozone chemistry scheme (Hsu and Prather, 2009). Although EAMv1 produces a quasi-biennial oscillation (QBO), it tends to be too strong and frequent compared to observations and can be greatly improved by modifying parameterized convectively generated gravity waves (Richter et al., 2019). As with the CanESM simulations, we consider both version 3 and 4 of the volcanic aerosol dataset, performing three simulations with each version.

4 Results

4.1 Radiative Forcing

Volcanic aerosols absorb near-infrared and thermal radiation, heating the stratosphere, while simultaneously cooling the troposphere due to scattering of visible and near-infrared radiation. The magnitude of this effect has been investigated in numerous studies, with marked decrease in radiation at the surface (Dutton and Christy, 1992) and tropopause (Hansen et al., 1992), and increases at the top of the atmosphere (Minnis et al., 1993; Stenchikov et al., 1998; Ramachandran et al., 2000). For this work, radiative forcing is computed as the instantaneous net outgoing flux at the top of the atmosphere for solar wavelengths (less than 4 microns) and thermal wavelengths (greater than 4 microns). Net total radiative forcing is calculated as the sum of the solar and thermal components.

Simulations were performed in atmosphere-only mode using sea-surface temperature and sea-ice prescribed by observations for the period 1990-1999 following the AMIP protocol (Gates et al., 1999). For this configuration an additional, diagnostic, atmospheric radiative transfer calculation is performed in which the stratospheric aerosol is zeroed out. The difference between the two computations then gives the instantaneous radiative forcing due to the presence of the stratospheric aerosols. Figure 3

5   shows the solar, thermal and net stratospheric aerosol radiative forcings from the version 3 and version 4 aerosol datasets for the global average and three latitude bands. The thermal forcing from the Pinatubo eruption peaks at approximately -2.5 Wm^{-2} in the tropics and -1.5 Wm^{-2} globally. Solar forcing is larger, peaking at nearly 6 and 3.7 Wm^{-2} for the tropics and global averages, respectively. Polar regions can also have large solar forcing during the summer months, but the smaller geographic area and seasonal cycle due to reduced solar insolation in the winter lead to only a small impact globally. Differences in radiative forcing

10   between version 3 and 4, shown as the shaded gray region, are much smaller, with net forcing differences peaking at 0.44 Wm^{-2} in the tropics and 0.11 Wm^{-2} globally. While maximum forcing differences in the SH polar regions are larger than the tropics (up to 1 Wm^{-2}), the relatively small area contributes little to the global averages.
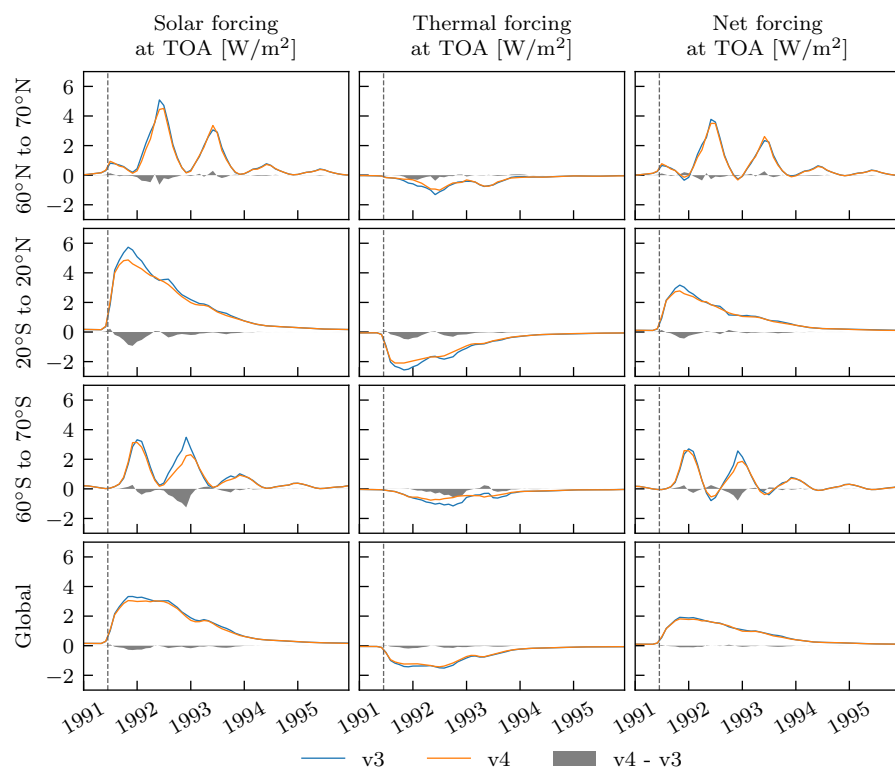
Figure 3. The left column shows the instantaneous solar radiative forcing at the top of atmosphere due to stratospheric aerosols in CanESM5. The blue line shows the forcing from version 3, the orange from version 4, and the gray shaded region indicates the difference in forcing between the two datasets (v4 -v3). The center column shows the instantaneous thermal radiative forcing at top of atmosphere, and the right column shows the instantaneous net radiative forcing at top of atmosphere. Each row shows the results for a different latitude band.

The absorption of both solar and thermal radiation heats the stratosphere in regions of enhanced aerosol loading (Kinne et al., 1992; Kinnison et al., 1994; Stenchikov et al., 1998; Andersen et al., 2001). Figure 4 shows the vertical distribution of instantaneous heating rates due to stratospheric aerosols computed using version 3 of the aerosol dataset. Tropical heating rates have been scaled by a factor of 1/3 so that tropical and extratropical heatings rates can be compared on the same color

5 axis. The largest heating rate of 0.5°C/day in the tropics near 24 km is seen approximately 6 months after the eruption, and contributes to a globally averaged instantaneous heating rate of 0.2°C/day, with increases over background that last until early 1994. The differences in instantaneous heating rates from version 3 to version 4 are also shown in Figure 4. At times, heating rates have been reduced in version 4 by almost half where extinction is largest, with slight increases in heating rates closer to the tropopause. This result is consistent with the differences between the aerosol datasets (Figure 2).
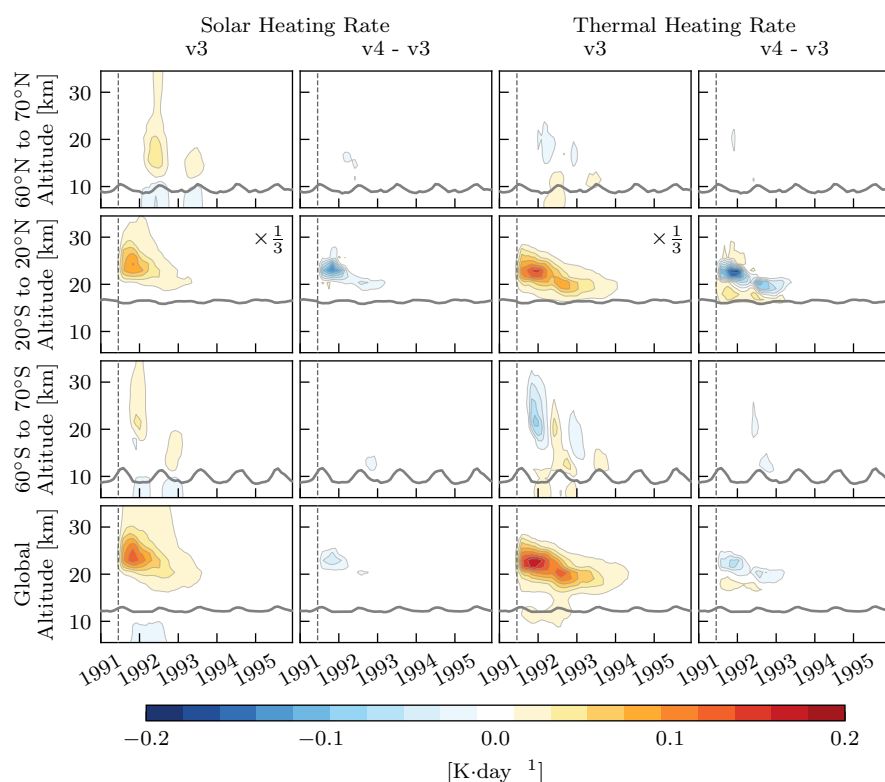
Figure 4. The left column shows the instantaneous solar heating rate due to stratospheric aerosols using the version 3 forcing dataset. The second column shows the change in the instantaneous solar heating rate when version 4 is used instead. The third and fourth columns show the same, expect for the instantaneous thermal heating rates. The gray lines denote the tropopause, and dashed lines indicate the date of the Pinatubo eruption. Note that the v3 instantaneous heating rates in the tropics have been multiplied by 1/3 for visual representation.

4.2 Climate Response

The radiative heating rates induced by volcanic eruptions translate to substantial warming in tropical stratospheric temperature anomalies in CMIP5 models, ranging from 2°C to nearly 10°C in the tropical stratosphere (Douglass and Knox, 2005; Driscoll et al., 2012; Arfeuille et al., 2013). To explore the climate response to volcanic forcing, transient historical experiments were

5   performed with CanESM5 following the methodologies set forth for CMIP6 (Eyring et al., 2016) using the version 3 aerosol climatology and all standard forcings. Simulations using version 4 of the stratospheric aerosol data were performed with the same protocol by branching new simulations off of CanESM5 historical simulations at the end of 1989. This was done for 15 realizations, with simulations using version 4 data run until 2014. In addition, three realizations were performed using the EAMv1 model. As with the CanESM5 instantaneous radiative forcing calculations, these simulations were performed using

10   the CMIP6 protocols (but for the AMIP experiment) for the period 1990-1999.

The ensemble mean CanESM5 stratospheric temperature anomalies following the Pinatubo eruption are shown in the left column of Figure 5. Temperature anomalies up to 7°C are seen in the tropics near 24 km, where the extinction, and solar heating rates are largest. The stratosphere also exhibits a long-term stratospheric cooling, but linearly detrending the record still results in a maximum temperature anomaly of 6°C, and does not change differences seen between version 3 and version 4. The

15   structure of the global averaged temperature anomaly largely follows the evolution of the tropical temperatures, but peaks at approximately 3°C, which results because temperature anomalies outside of the tropics are considerably smaller. When using version 4 of the stratospheric aerosol data the peak temperature anomalies in the tropics are reduced by just over 2°C, and peak global anomalies are reduced by 0.8°C. The stratospheric temperature response in the polar regions can differ by 2-4°C, depending on the version of the SAOD used, but these differences are considerably smaller than the between-realization vari-

20   ability, which has a standard deviation of 6°C in these regions. Increases in stratospheric temperature as modelled by EAMv1 are similar in magnitude (see Figure S1). However, with only three ensemble members, temperature differences compared to version 4 are not statistically significant at the 95% level.
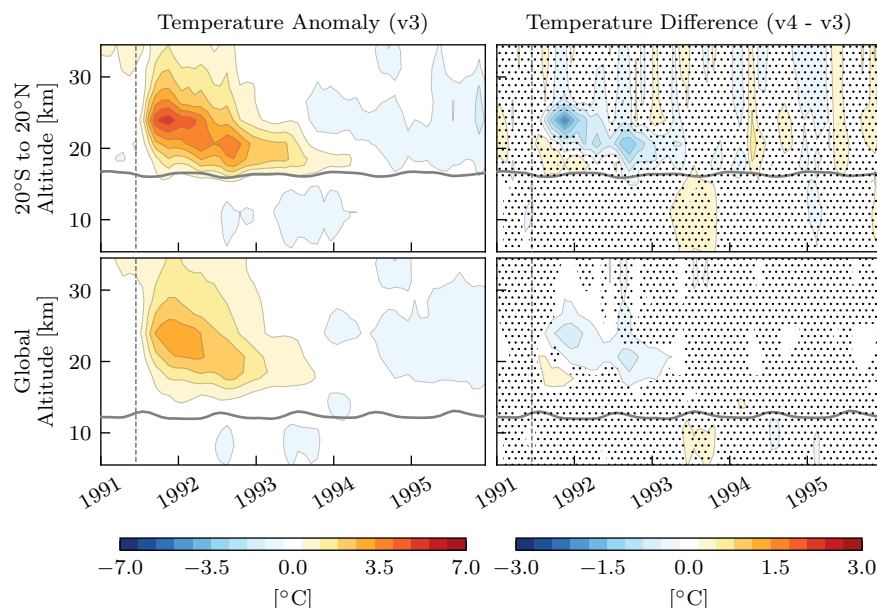
Figure 5. The left column shows the monthly temperature anomalies averaged over all CanESM5 ensemble members with version 3 forcing for 20°S to 20°N (top) and the global average (bottom). The right column shows the difference in temperature when using the version 3 and version 4 datasets. Stippling marks the regions where differences are not significantly different from zero at the 95% confidence level. Anomalies are computed using the simulation period of 1990 through 1999.

For observational comparisons data from the Remote Sensing Systems (RSS) microwave temperature record (Mears and Wentz, 2009; Mears and Wentz, 2009) is used. The RSS datasets are composed of measurements from the Microwave Sounding Units and Advanced Microwave Sounding Units which provide temperature information for several deep atmospheric layers. For this study, the temperature of the lower stratosphere (TLS) and temperature of the lower Troposphere (TLT) products are

5   used. TLS is a weighted average from approximately 10 to 30 km, with a peak sensitivity at 17.4 km and 75% of the contribution coming from between 14 to 22 km. TLT data is from below 10 km with over 75% of the signal from below 5.5 km including a 10-15% contribution from the surface (Mears and Wentz, 2017). Comparable temperature records from CanESM5 and EAMv1 are computed by applying RSS weighting functions to model temperatures. Since TLT includes a significant contribution from the surface, the weighting function depends on the surface type (land or ocean) to account for surface emissivity differences.

10   Figure 6 shows TLS and TLT anomalies simulated by CanESM5 and EAMv1 using version 3 and version 4 of the dataset in blue and orange respectively, as well as the RSS measurements in black. TLS anomalies are smaller in version 4 by up to 0.5°C in the tropics and 0.25°C globally, but modelled TLS values still remain approximately 1°C above measured values when globally averaged. This model-observational difference in stratospheric temperature has also been noted in other GCMs (Lanzante and Free, 2008; Gettelman et al., 2010). EAMv1 stratospheric temperatures in the tropics show increased variability

15   when compared to CanESM5 due to the quasi-biennial oscillation, which is not present in CanESM5. Tropospheric temperature differences arising from changes to the aerosol dataset are smaller than in the stratosphere for both models. EAMv1 results

exhibit much smaller variability between ensemble members in the lower troposphere due to specified sea surface temperatures, and do not show a significant difference between versions 3 and 4. CanESM5 differences in TLT of approximately 0.2°C in the tropics and 0.1°C globally are present in 1993, but result primarily from a change in the phase of the El Niño Southern Oscillation (ENSO) between version 3 and version 4 runs.
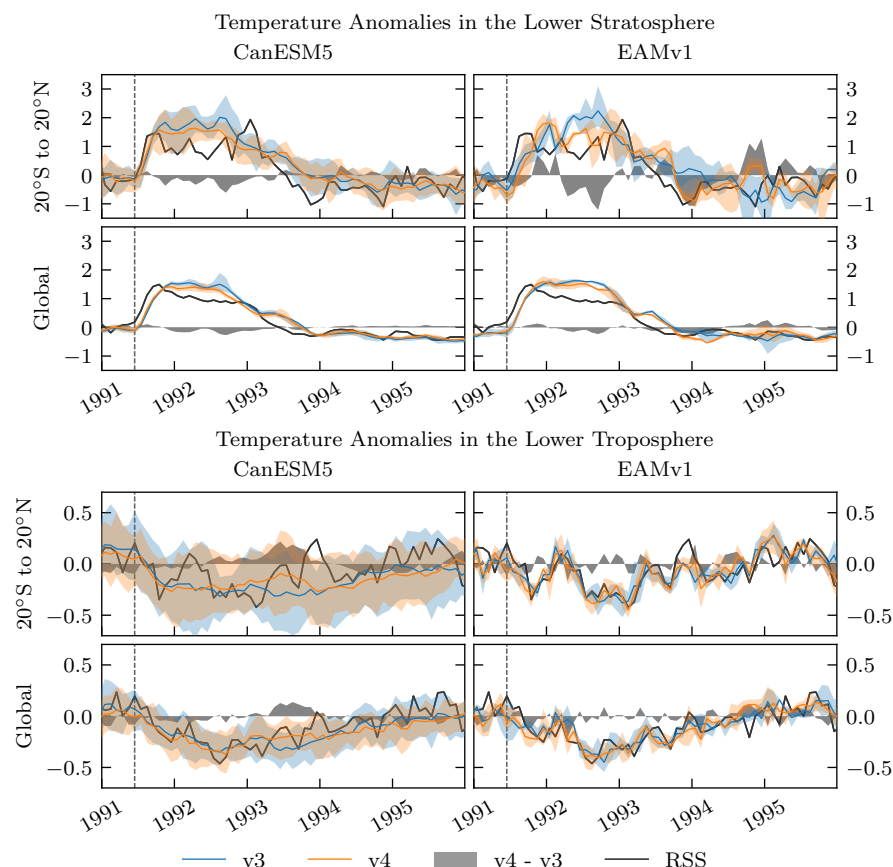
Figure 6. Temperature anomalies in the lower stratosphere (top two rows) and lower troposphere (bottom two rows) in the tropics and globally averaged. The left column shows results from CanESM5 and the right column EAMv1. Solid blue lines show the mean temperature anomaly using the version 3 dataset and orange show the same using version 4. The blue and orange shaded regions show the 10th and 90th percentiles for version 3 and 4 respectively for the CanESM5 ensemble and the max/min range for the EAMv1 ensemble. The gray region shows the mean difference between simulations using version 3 and version 4. The black line shows the RSS observations and the dashed line marks the eruption of Pinatubo on June 15th, 1991. Anomalies are computed using the simulation period of 1990 through 1999.

5   While large eruptions may increase the likelihood and magnitude of El Niño events (Adams et al., 2003; Mann et al., 2005; Emile-Geay et al., 2008), the response is heavily model dependent (Predybaylo et al., 2017). Due to non-zero changes in the volcanic forcing before the eruption, the version 3 and version 4 ensembles are not in the same internal state on June 16th when Pinatubo erupts, with the version 4 ensemble tending slightly to more La Niña-like states. This can have a marked effect on

the climate response (Pausata et al., 2016; Zanchettin et al., 2019). However, there is no apparent difference in ENSO states in the 2 years following the eruption when initial conditions are taken into account. Additionally, changes to the aerosol forcing do not have a significant impact on ocean heat content, as shown in Figure 7. As such, changes to atmospheric temperatures in CanESM5 AMIP runs (not shown) show comparable changes to coupled runs, and therefore the AMIP runs from the EAMv1

5   model are expected to be a good representation of results from the coupled model.
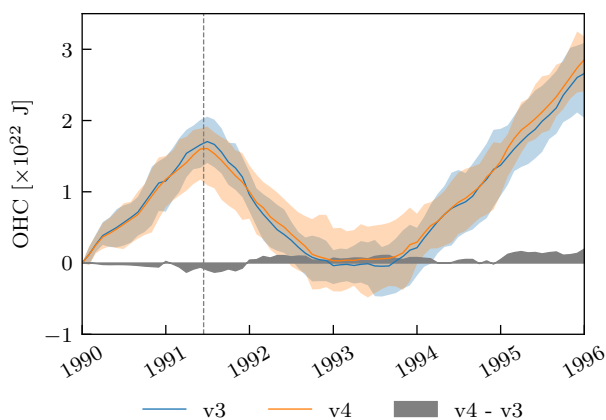
Figure 7. Monthly deseasonalized ocean heat content relative to January 1990. The blue line shows OHC using the version 3 aerosol forcing while the orange line indicates results when using version 4. The shading indicates the 10th and 90th percentiles of the data.

In addition to temperature responses, several studies have noted a decrease in global precipitation following the Pinatubo eruption (Robock and Liu, 1994; Broccoli et al., 2003; Gillett et al., 2004; Barnes et al., 2016). The CanESM5 ensemble mean shows a global precipitation decrease of 0.05 mm/day one year after the eruption, consistent with previous studies. However, this is similar for both the version 3 and version 4 datasets, and differences in precipitation due to the change in stratospheric

10 aerosols are not statistically significant. These results are summarized in Figure 8 that shows the changes in climate response when using version 3 and version 4 aerosols averaged for two years following the Pinatubo eruption. For CanESM5, with results shown as the box and whisker plots, the largest differences in temperatures between aerosol datasets occur near 24 km and are statistically significant from zero at the 95% confidence level, as are the changes in the TLS. Changes in lower tropospheric temperatures are not statistically significant between versions, nor are changes in precipitation. EAMv1 results are shown as

15 individual points, and indicate similar responses to those seen in CanESM5.
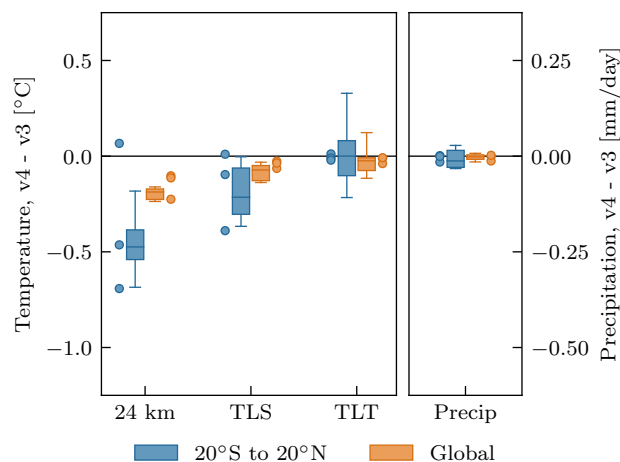
Figure 8. Difference in temperature and precipitation levels between version 3 and version 4 for the 2 years following the Pinatubo eruption. Boxes show the interquartile range of the CanESM5 data from the 15 member ensemble, and whiskers mark the 10th and 90th percentiles. Individual markers show the values from each of the three EAMv1 ensemble realizations.

5 Conclusions

Since publication of the version 3 stratospheric aerosol dataset recommended for CMIP6, updates included in version 4 have resulted in extinction differences as large 50% in the aerosol plume of the Pinatubo eruption. When these datasets are used in CanESM5 it is found that using version 4 instead of version 3 caused reductions in the instantaneous top-of-atmosphere

5 radiative fluxes up to $0.44\,\mathrm{W/m^2}$ in the tropics approximately 6 months following the eruption and maximum differences in instantaneous radiative heating rates of $0.2\,^\circ$C/day in the tropics. The substantial change in stratospheric heating rates at specific altitudes following the eruption results in significant temperature response differences of up to 3°C. Over deeper layers and larger spatial scales the impact is less pronounced with only the TLS showing statistical significance. As a result, the impact on global precipitation rates is also small. Temperatures in the lower stratosphere, between approximately 14 and 22 km, are

10 decreased by 0.2°C with no statistically significant change in the lower troposphere. Similarly, precipitation rates and changes to the ENSO index are not substantial enough to be distinguished from unforced internal model variability. Based on results from two models participating in CMIP6, we find that the impact of the update from version 3 to version 4 of the stratospheric aerosol dataset is relatively small for the fields considered of radiative forcing, temperature, and precipitation. This indicates that while there is a known forcing issue in the v3 stratospheric aerosol dataset, this does not undermine the utility of the

15 CMIP6 historical ensemble to quantify the anthropogenic-forced impact on the climate. Use of the new SAOD dataset may, however, affect quantities not considered in this study, and its impact may be model dependent, so modelling groups interested in the post-Pinatubo response may want to assess the impact of the new SAOD dataset in their models.

Code and data availability. The CanESM5 model code is available at https://gitlab.com/cccma/canesm. CanESM5 model data and analysis code is available at 10.5281/zenodo.3524445. The E3SM project, code, simulation configurations, model output, and tools to work with the output are described at the E3SM website (https://e3sm.org). Instructions on how to get started running E3SM and its components are available at the E3SM website (https://e3sm.org/model/running-e3sm/e3sm-quick-start). All model codes may be accessed on the GitHub

5   repository (at https://github.com/E3SM-Project/E3SM)

Author contributions. LR, JCN, JCF and NPG contributed to the manuscript writing, preparation and design of the CanESM5 experiments. SP contributed to the manuscript writing, preparation and design of the E3SM experiments. PJD, PJC-S and QT contributed to the design of E3SM experiments and reviewed the manuscript.

Competing interests. The authors declare that they have no conflict of interest.

10   *Acknowledgements.* Work performed by S. Po-Chedley, P. J. Cameron-Smith, P. J. Durack, and Q. Tang at Lawrence Livermore National Laboratory (LLNL) was under the auspices of the U.S. Department of Energy under Contract DE-AC52-07NA27344. S. Po-Chedley was funded by LLNL LDRD 18-ERD-054. The work of P. J. Cameron-Smith and Q. Tang was under the Energy Earth System Model (E3SM) project, which is funded by the U.S. Department of Energy, Office of Science, Office of Biological and Environmental Research. NCEP Reanalysis data provided by the NOAA/OAR/ESRL PSD, Boulder, Colorado, USA, from their web site at https://www.esrl.noaa.gov/psd/. The

15   authors would also like to thank Benjamin Santer, James Anstey and Adam Bourassa for comments on the manuscript and the development teams of E3SM and CanESM5.

References

Adams, J. B., Mann, M. E., and Ammann, C. M.: Proxy evidence for an El Nino-like response to volcanic forcing, Nature, 426, 274, 2003.

Ammann, C. M., Meehl, G. A., Washington, W. M., and Zender, C. S.: A monthly and latitudinally varying volcanic forcing dataset in simulations of 20th century climate, Geophysical Research Letters, 30, 2003.

5 Andersen, U. J., Kaas, E., and Alpert, P.: Using analysis increments to estimate atmospheric heating rates following volcanic eruptions, Geophysical research letters, 28, 991–994, 2001.

Andersson, S. M., Martinsson, B. G., Vernier, J.-P., Friberg, J., Brenninkmeijer, C. A., Hermann, M., Van Velthoven, P. F., and Zahn, A.: Significant radiative impact of volcanic aerosol in the lowermost stratosphere, Nature communications, 6, 7692, 2015.

Arfeuille, F., Luo, B., Heckendorn, P., Weisenstein, D., Sheng, J., Rozanov, E., Schraner, M., Brönnimann, S., Thomason, L., and Peter, T.:
10 Modeling the stratospheric warming following the Mt. Pinatubo eruption: uncertainties in aerosol extinctions, Atmospheric chemistry and physics, 13, 11 221–11 234, 2013.

Barnes, E. A., Solomon, S., and Polvani, L. M.: Robust wind and precipitation responses to the Mount Pinatubo eruption, as simulated in the CMIP5 models, Journal of Climate, 29, 4763–4778, 2016.

Broccoli, A. J., Dixon, K. W., Delworth, T. L., Knutson, T. R., Stouffer, R. J., and Zeng, F.: Twentieth-century temperature and precipitation
15 trends in ensemble climate simulations including natural and anthropogenic forcing, Journal of Geophysical Research: Atmospheres, 108, 2003.

Church, J. A., White, N. J., and Arblaster, J. M.: Significant decadal-scale impact of volcanic eruptions on sea level and ocean heat content, Nature, 438, 74, 2005.

Douglass, D. H. and Knox, R. S.: Climate forcing by the volcanic eruption of Mount Pinatubo, Geophysical Research Letters, 32,
20 https://doi.org/10.1029/2004GL022119, https://agupubs.onlinelibrary.wiley.com/doi/abs/10.1029/2004GL022119, 2005.

Driscoll, S., Bozzo, A., Gray, L. J., Robock, A., and Stenchikov, G.: Coupled Model Intercomparison Project 5 (CMIP5) simulations of climate following volcanic eruptions, Journal of Geophysical Research: Atmospheres, 117, 2012.

Durack, P., Taylor, K., Eyring, V., Ames, S., Hoang, T., Nadeau, D., Doutriaux, C., Stockhause, M., and Gleckler, P.: Toward standardized data sets for climate model experimentation, Eos, 99, 2018.

25 Durack, P. J. and Taylor, K. E.: PCMDI AMIP SST and sea-ice boundary conditions version 1.1.3, https://doi.org/10.22033/ESGF/input4MIPs.1735, https://doi.org/10.22033/ESGF/input4MIPs.1735, 2017.

Dutton, E. G. and Christy, J. R.: Solar radiative forcing at selected locations and evidence for global lower tropospheric cooling following the eruptions of El Chichón and Pinatubo, Geophysical Research Letters, 19, 2313–2316, 1992.

Emile-Geay, J., Seager, R., Cane, M. A., Cook, E. R., and Haug, G. H.: Volcanoes and ENSO over the past millennium, Journal of Climate,
30 21, 3134–3148, 2008.

Eyring, V., Bony, S., Meehl, G. A., Senior, C. A., Stevens, B., Stouffer, R. J., and Taylor, K. E.: Overview of the Coupled Model Intercomparison Project Phase 6 (CMIP6) experimental design and organization, Geoscientific Model Development, 9, 1937–1958, https://doi.org/10.5194/gmd-9-1937-2016, https://www.geosci-model-dev.net/9/1937/2016/, 2016.

Fyfe, J., Von Salzen, K., Cole, J., Gillett, N., and Vernier, J.-P.: Surface response to stratospheric aerosol changes in a coupled atmosphere–
35 ocean model, Geophysical Research Letters, 40, 584–588, 2013.

Gates, W. L., Boyle, J. S., Covey, C., Dease, C. G., Doutriaux, C. M., Drach, R. S., Fiorino, M., Gleckler, P. J., Hnilo, J. J., Marlais, S. M., Phillips, T. J., Potter, G. L., Santer, B. D., Sperber, K. R., Taylor, K. E., and Williams, D. N.: An Overview of the Results of the Atmospheric

Model Intercomparison Project (AMIP I), Bulletin of the American Meteorological Society, 80, 29–56, https://doi.org/10.1175/1520-0477(1999)080<0029:AOOTRO>2.0.CO;2, https://doi.org/10.1175/1520-0477(1999)080<0029:AOOTRO>2.0.CO;2, 1999.

Gettelman, A., Hegglin, M. I., Son, S.-W., Kim, J., Fujiwara, M., Birner, T., Kremser, S., Rex, M., Añel, J., Akiyoshi, H., et al.: Multimodel assessment of the upper troposphere and lower stratosphere: Tropics and global trends, Journal of Geophysical Research: Atmospheres,
5   115, 2010.

Gillett, N., Weaver, A., Zwiers, F., and Wehner, M.: Detection of volcanic influence on global precipitation, Geophysical Research Letters, 31, 2004.

Golaz, J.-C., Caldwell, P. M., Van Roekel, L. P., Petersen, M. R., Tang, Q., Wolfe, J. D., Abeshu, G., Anantharaj, V., Asay-Davis, X. S., Bader, D. C., Baldwin, S. A., Bisht, G., Bogenschutz, P. A., Branstetter, M., Brunke, M. A., Brus, S. R., Burrows, S. M., Cameron-Smith,
10   P. J., Donahue, A. S., Deakin, M., Easter, R. C., Evans, K. J., Feng, Y., Flanner, M., Foucar, J. G., Fyke, J. G., Griffin, B. M., Hannay, C., Harrop, B. E., Hoffman, M. J., Hunke, E. C., Jacob, R. L., Jacobsen, D. W., Jeffery, N., Jones, P. W., Keen, N. D., Klein, S. A., Larson, V. E., Leung, L. R., Li, H.-Y., Lin, W., Lipscomb, W. H., Ma, P.-L., Mahajan, S., Maltrud, M. E., Mametjanov, A., McClean, J. L., McCoy, R. B., Neale, R. B., Price, S. F., Qian, Y., Rasch, P. J., Reeves Eyre, J. E. J., Riley, W. J., Ringler, T. D., Roberts, A. F., Roesler, E. L., Salinger, A. G., Shaheen, Z., Shi, X., Singh, B., Tang, J., Taylor, M. A., Thornton, P. E., Turner, A. K., Veneziani, M., Wan, H., Wang, H.,
15   Wang, S., Williams, D. N., Wolfram, P. J., Worley, P. H., Xie, S., Yang, Y., Yoon, J.-H., Zelinka, M. D., Zender, C. S., Zeng, X., Zhang, C., Zhang, K., Zhang, Y., Zheng, X., Zhou, T., and Zhu, Q.: The DOE E3SM Coupled Model Version 1: Overview and Evaluation at Standard Resolution, Journal of Advances in Modeling Earth Systems, 11, 2089–2129, https://doi.org/10.1029/2018MS001603, 2019.

Guo, S., Bluth, G. J., Rose, W. I., Watson, I. M., and Prata, A.: Re-evaluation of SO2 release of the 15 June 1991 Pinatubo eruption using ultraviolet and infrared satellite sensors, Geochemistry, Geophysics, Geosystems, 5, 2004.

20   Hansen, J., Lacis, A., Ruedy, R., and Sato, M.: Potential climate impact of Mount Pinatubo eruption, Geophysical Research Letters, 19, 215–218, 1992.

Haywood, J. M., Jones, A., and Jones, G. S.: The impact of volcanic eruptions in the period 2000–2013 on global mean temperature trends evaluated in the HadGEM2-ES climate model, Atmospheric Science Letters, 15, 92–96, 2014.

Hsu, J. and Prather, M. J.: Stratospheric variability and tropospheric ozone, Journal of Geophysical Research: Atmospheres, 114, 2009.

25   Hurrell, J. W., Hack, J. J., Shea, D., Caron, J. M., and Rosinski, J.: A New Sea Surface Temperature and Sea Ice Boundary Dataset for the Community Atmosphere Model, Journal of Climate, 21, 5145–5153, https://doi.org/10.1175/2008JCLI2292.1, 2008.

Kalnay, E., Kanamitsu, M., Kistler, R., Collins, W., Deaven, D., Gandin, L., Iredell, M., Saha, S., White, G., Woollen, J., et al.: The NCEP/NCAR 40-year reanalysis project, Bulletin of the American meteorological Society, 77, 437–472, 1996.

Kinne, S., Toon, O. B., and Prather, M. J.: Buffering of stratospheric circulation by changing amounts of tropical ozone a Pinatubo Case
30   Study, Geophysical Research Letters, 19, 1927–1930, https://doi.org/10.1029/92GL01937, https://agupubs.onlinelibrary.wiley.com/doi/abs/10.1029/92GL01937, 1992.

Kinnison, D. E., Grant, K. E., Connell, P. S., Rotman, D. A., and Wuebbles, D. J.: The chemical and radiative effects of the Mount Pinatubo eruption, Journal of Geophysical Research: Atmospheres, 99, 25 705–25 731, 1994.

Kremser, S., Thomason, L. W., Hobe, M., Hermann, M., Deshler, T., Timmreck, C., Toohey, M., Stenke, A., Schwarz, J. P., Weigel, R., et al.:
35   Stratospheric aerosol—Observations, processes, and impact on climate, Reviews of Geophysics, 54, 278–335, 2016.

Lanzante, J. R. and Free, M.: Comparison of radiosonde and GCM vertical temperature trend profiles: effects of dataset choice and data homogenization, Journal of Climate, 21, 5417–5435, 2008.

Luo, B.: Stratospheric aerosol data for use in CMIP6 models, ftp://iacftp.ethz.ch/pub_read/luo/CMIP6/Readme_Data_Description.pdf, [Online; accessed 12-August-2019], 2018a.

Luo, B.: Release Notes Stratospheric Aerosol Radiative Forcing and SAD version v4.0.01850 - 2016, ftp://iacftp.ethz.ch/pub_read/luo/CMIP6_SAD_radForcing_v4.0.0/Release_note_v4.0.0.pdf, [Online; accessed 12-August-2019], 2018b.

5 Madec, G. and Imbard, M.: NEMO ocean engine, version 3.4, 27, Institut Pierre-Simon Laplace, 2012.

Mann, M. E., Cane, M. A., Zebiak, S. E., and Clement, A.: Volcanic and solar forcing of the tropical Pacific over the past 1000 years, Journal of Climate, 18, 447–456, 2005.

Mears, C. A. and Wentz, F. J.: Construction of the Remote Sensing Systems V3.2 atmospheric temperature records from the MSU and AMSU microwave sounders, Journal of Atmospheric and Oceanic Technology, 26, 1040–1056, 2009.

10 Mears, C. A. and Wentz, F. J.: Construction of the RSS V3.2 Lower-Tropospheric Temperature Dataset from the MSU and AMSU Microwave Sounders, Journal of Atmospheric and Oceanic Technology, 26, 1493, https://doi.org/10.1175/2009JTECHA1237.1, 2009.

Mears, C. A. and Wentz, F. J.: A satellite-derived lower-tropospheric atmospheric temperature dataset using an optimized adjustment for diurnal effects, Journal of Climate, 30, 7695–7718, 2017.

Minnis, P., Harrison, E. F., Stowe, L. L., Gibson, G., Denn, F. M., Doelling, D., and Smith, W.: Radiative climate forcing by the Mount
15 Pinatubo eruption, Science, 259, 1411–1415, 1993.

Pausata, F. S. R., Karamperidou, C., Caballero, R., and Battisti, D. S.: ENSO response to high-latitude volcanic eruptions in the Northern Hemisphere: The role of the initial conditions, Geophysical Research Letters, 43, 8694–8702, https://doi.org/10.1002/2016GL069575, https://agupubs.onlinelibrary.wiley.com/doi/abs/10.1002/2016GL069575, 2016.

Predybaylo, E., Stenchikov, G. L., Wittenberg, A. T., and Zeng, F.: Impacts of a Pinatubo-size volcanic eruption on ENSO, Journal of
20 Geophysical Research: Atmospheres, 122, 925–947, https://doi.org/10.1002/2016JD025796, https://agupubs.onlinelibrary.wiley.com/doi/abs/10.1002/2016JD025796, 2017.

Ramachandran, S., Ramaswamy, V., Stenchikov, G. L., and Robock, A.: Radiative impact of the Mount Pinatubo volcanic eruption: Lower stratospheric response, Journal of Geophysical Research: Atmospheres, 105, 24 409–24 429, 2000.

Rasch, P. J., Xie, S., Ma, P.-L., Lin, W., Wang, H., Tang, Q., Burrows, S. M., Caldwell, P., Zhang, K., Easter, R. C., Cameron-Smith, P.,
25 Singh, B., Wan, H., Golaz, J.-C., Harrop, B. E., Roesler, E., Bacmeister, J., Larson, V. E., Evans, K. J., Qian, Y., Taylor, M., Leung, L. R., Zhang, Y., Brent, L., Branstetter, M., Hannay, C., Mahajan, S., Mametjanov, A., Neale, R., Richter, J. H., Yoon, J.-H., Zender, C. S., Bader, D., Flanner, M., Foucar, J. G., Jacob, R., Keen, N., Klein, S. A., Liu, X., Salinger, A., Shrivastava, M., and Yang, Y.: An Overview of the Atmospheric Component of the Energy Exascale Earth System Model, Journal of Advances in Modeling Earth Systems, 11, https://doi.org/10.1029/2019MS001629, https://agupubs.onlinelibrary.wiley.com/doi/abs/10.1029/2019MS001629, 2019.

30 Richter, J. H., Chen, C.-C., Tang, Q., Xie, S., and Rasch, P. J.: Improved Simulation of the QBO in E3SMv1, Journal of Advances in Modeling Earth Systems, 11, 3403–3418, https://doi.org/10.1029/2019MS001763, https://agupubs.onlinelibrary.wiley.com/doi/abs/10.1029/2019MS001763, 2019.

Ridley, D., Solomon, S., Barnes, J., Burlakov, V., Deshler, T., Dolgii, S., Herber, A. B., Nagai, T., Neely III, R., Nevzorov, A., et al.: Total volcanic stratospheric aerosol optical depths and implications for global climate change, Geophysical Research Letters, 41, 7763–7769,
35 2014.

Robock, A. and Liu, Y.: The volcanic signal in Goddard Institute for Space Studies three-dimensional model simulations, Journal of Climate, 7, 44–55, 1994.

Robock, A. and Mao, J.: The volcanic signal in surface temperature observations, Journal of Climate, 8, 1086–1103, 1995.

Santer, B. D., Bonfils, C., Painter, J. F., Zelinka, M. D., Mears, C., Solomon, S., Schmidt, G. A., Fyfe, J. C., Cole, J. N., Nazarenko, L., et al.: Volcanic contribution to decadal changes in tropospheric temperature, Nature Geoscience, 7, 185, 2014.

Sato, M., Hansen, J. E., McCormick, M. P., and Pollack, J. B.: Stratospheric aerosol optical depths, 1850–1990, Journal of Geophysical Research: Atmospheres, 98, 22 987–22 994, 1993.

5   Solomon, S., Daniel, J. S., Neely, R. R., Vernier, J.-P., Dutton, E. G., and Thomason, L. W.: The persistently variable "background" stratospheric aerosol layer and global climate change, Science, 333, 866–870, 2011.

Stenchikov, G. L., Kirchner, I., Robock, A., Graf, H.-F., Antuna, J. C., Grainger, R., Lambert, A., and Thomason, L.: Radiative forcing from the 1991 Mount Pinatubo volcanic eruption, Journal of Geophysical Research: Atmospheres, 103, 13 837–13 857, 1998.

Swart, N. C., Cole, J. N. S., Kharin, V. V., Lazare, M., Scinocca, J. F., Gillett, N. P., Anstey, J., Arora, V., Christian, J. R., Hanna, S., Jiao, Y.,
10   Lee, W. G., Majaess, F., Saenko, O. A., Seiler, C., Seinen, C., Shao, A., Solheim, L., von Salzen, K., Yang, D., and Winter, B.: The Canadian Earth System Model version 5 (CanESM5.0.3), Geoscientific Model Development Discussions, 2019, 1–68, https://doi.org/10.5194/gmd-2019-177, https://www.geosci-model-dev-discuss.net/gmd-2019-177/, 2019.

Taylor, K. E., Stouffer, R. J., and Meehl, G. A.: An overview of CMIP5 and the experiment design, Bulletin of the American Meteorological Society, 93, 485–498, 2012.

15   Thomason, L. W., Ernest, N., Millán, L., Rieger, L., Bourassa, A., Vernier, J.-P., Manney, G., Luo, B., Arfeuille, F., and Peter, T.: A global space-based stratospheric aerosol climatology: 1979-2016, Earth System Science Data, 10, 469–492, 2018.

Thompson, D. W. and Solomon, S.: Understanding recent stratospheric climate change, Journal of Climate, 22, 1934–1943, 2009.

Vernier, J.-P., Thomason, L. W., Pommereau, J.-P., Bourassa, A., Pelon, J., Garnier, A., Hauchecorne, A., Blanot, L., Trepte, C., Degenstein, D., et al.: Major influence of tropical volcanic eruptions on the stratospheric aerosol layer during the last decade, Geophysical Research
20   Letters, 38, 2011.

Zanchettin, D., Timmreck, C., Toohey, M., Jungclaus, J. H., Bittner, M., Lorenz, S. J., and Rubino, A.: Clarifying the Relative Role of Forcing Uncertainties and Initial-Condition Unknowns in Spreading the Climate Response to Volcanic Eruptions, Geophysical Research Letters, 46, 1602–1611, 2019.